The Crystal Structure and Raman Spectrum of the Sodium Salt of 5-Acetic Acid Hydantoin

Bernardo A. Nogueira,[1,*] Gulce O. Ildiz,[1,2] Andreia M. Tabanez,[1]

M. S. C. Henriques,[3] José A. Paixão[3] and Rui Fausto[1]

[1] *University of Coimbra, CQC, Department of Chemistry, P-3004-535 Coimbra, Portugal.*
[2] *Faculty of Sciences and Letters, Department of Physics, Istanbul Kultur University, Atakoy Campus, Bakirkoy 34156, Istanbul, Turkey.*
[3] *University of Coimbra, CFisUC, Department of Physics, P-3004-516 Coimbra, Portugal.*

Abstract

The sodium salt of 5-acetic acid hydantoin (5AAH) was synthesized, and its crystal structure determined by single crystal X-ray diffraction. The material was found to exhibit rather unusual structural features. Firstly, contrarily to what is most common for hydantoins, the 5AAH molecules in the crystal bind the sodium ions through coordination *via* its oxygen atoms (instead of *via* a deprotonated ring nitrogen). In second place, the molecular formula of the salt is $Na(5AAH)_2$, i.e., the formal charge of the hydantoin in the crystal is −0.5 *e*. Finally, the conformation adopted by the 5AAH molecules in the crystal of the salt is neither the most stable conformer for the isolated molecule (and observed before in the gas phase of the compound), nor that present in the neat crystalline compound (most stable polymorph at room temperature). These results show that 5AAH is a structurally very versatile molecule, which is able to participate in strong intermolecular interactions that can supersede the intrinsic higher structural stability of the individual molecules and lead to selection of different higher energy conformers on formation of a crystalline phase.

The Raman spectrum of the newly synthesized salt was also obtained and used to extract further structural details of the crystal, in particular on the prevalent intermolecular interactions. The results (both structural and spectroscopic) obtained for the studied sodium salt of 5AAH are also compared with those relative to the neat 5AAH most stable crystalline polymorph at room temperature. To help the interpretation of the spectra, DFT(B3LYP)/6-311++G(d,p) calculations were undertaken on simple models based on the structural elements of the crystals.

Keywords: 5-acetic acid hydantoin sodium salt; Single crystal X-ray diffraction; Raman spectroscopy; DFT calculations.

**** Corresponding author e-mail:*** ban@qui.uc.pt

Introduction

Hydantoins have many practical uses. They receive application as pharmaceuticals (*e.g.*, phenytoin and fosphenytoin are used as anticonvulsants in the treatment of seizures and epilepsy [1-4], dantrolene is used as a muscle relaxant to treat, for instance, spasticity and ecstasy intoxication [5,6], and ropitoin is used as an antiarrhythmic drug [7], while several hydantoin derivatives have also been proposed for the treatment of cancer and AIDS [8-11]), as desinfectants, insecticides, herbicides and fungicides (as, for example, sulfochloranthine, imiprothrin and iprodione [12-14]), and as reactants in the synthesis of amino acids [15,16]. 5-acetic acid hydantoin (2-(2,5-dioxoimidazolidin-4-yl)acetic acid; abbreviated 5AAH; Fig. 1) has been shown to have antitumor activity [17] and is used in the synthesis of anti-inflammatory and analgesic active compounds [18]. Knowledge on details of the molecular structure for the isolated hydantoin molecules or for their condensed phases is instrumental to understand their mechanisms of action at the different levels and areas of application of the compounds.

Within the scope of our research programme on hydantoin derivatives [19-24], we have recently shown that 5AAH exhibits five different polymorphs, from which the most stable one at room temperature (polymorph I) has the peculiar characteristic of being formed by 5AAH molecules that assume a conformation identical to the highest-energy conformer for the isolated molecule [24]. In fact, this higher-energy conformer, which has an energy as large as ~40 kJ mol^{-1} higher than that of the conformational ground state, is selected upon crystallization from among 13 different conformers of the molecule. The selection upon crystallization of a conformer that for the isolated molecule is not the absolute minimum energy structure is not a rare phenomenon [25], however, this is an extreme case that, to the best of our knowledge, has no parallel in the literature.

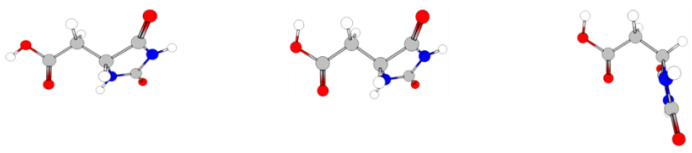

Figure 1. Experimentally relevant conformers of 5AAH. From left to right: *cis*-**I**, the most stable conformer for the isolated molecule and observed experimentally for the compound isolated in cryogenic inert matrices [24]; *trans*-**I**, the conformer present in the investigated sodium salt of 5AAH; *trans*-**III**, the conformer present in the room temperature most stable crystal (polymorph I) of the neat hydantoin [24]. On total, the molecule has 13 different conformers [24]. The numbers in parentheses are the DFT(B3LYP)/6-311++G(d,p) calculated relative energies of the conformers [24].

In the present study we focused our attention on the sodium salt of 5AAH, which had never been investigated before. Our interest for this system resulted mostly from our curiosity to answer the following questions:

(i) Does 5AAH coordinate sodium ions *via* the hydantoin ring (through a deprotonated ring nitrogen atom as it in general occurs for hydantoins, *e.g.* phenytoin [26]) or through the carboxylic acid substituent?

(ii) Which is the protonation state of the 5AAH in the complex?

(iii) Which is the conformation assumed by the 5AAH molecules in the complex?

We were particularly interested to determine the conformational preferences of the 5AAH molecules in the crystal of the newly synthesized salt, and compare the results with what has been observed for the neat hydantoin [24]. We were also very much interested to compare the crystal structures of the hydantoin and of its salt regarding the most relevant intermolecular interactions defining their structures, in particular hydrogen bonding.

As it will be shown in details below, the sodium salt of 5AAH was found to exhibit a stunning crystal structure where (a) all carbonyl moieties present in the 5AAH molecules coordinate a sodium ion while both nitrogen atoms of the hydantoin ring are protonated, (b) the effective charge of the ligand is –0.5 *e*, with the carboxylic hydrogen atom being equally shared by two hydantoin molecules, and (c) the conformation adopted by the hydantoin molecules is different from that found in the known crystal of the neat hydantoin, but it is still a high-energy form for the isolated molecule of the compound.

Besides the crystallographic study, we present also the Raman spectrum of the salt and interpret it in comparison with the spectrum of the crystalline hydantoin (polymorph I [24]), taking into account the X-ray diffraction structural information now determined for the salt and that previously reported for the ligand [24]. The analysis of the Raman spectroscopy data is also supported by theoretical results obtained within the scope of the density functional theory (DFT).

Experimental Procedures and Computational Methods

The sodium salt of 5-acetic acid hydantoin, with formula $C_{10}H_{11}N_4NaO_8$, was synthesized from the hydantoin (35 mg) and NaOH in dioxane solution (4 mL). The solvent was let to

evaporate slowly at room temperature and the resulting material was subsequently dried in a desiccator for several days. Examination at the microscope showed that the obtained material was a mixture of two crystals, with clearly different morphologies. The Raman spectra of the two types of crystals allowed to conclude that those present in larger amount corresponded to the original hydantoin, while those present in smaller quantity should be assigned to a new material, which, as demonstrated by single crystal X-ray diffraction, was found to be the sodium salt of 5AAH.

Raman spectra (in the 50-4000 cm^{-1} range) were registered with accuracy better than 0.5 cm^{-1} using a micro-Raman system Horiba LabRam HR Evolution. A HeNe laser (λ = 633 nm; *P*= ~17 mW at the sample), a collection time of 30 seconds, 30 accumulations, and a 50x objective (laser spot diameter of 1 μm at the sample) were used. Wavenumber calibration was done using the Si wafer band at 520.5 cm^{-1}.

The single crystal X-ray diffraction experiments were performed at room temperature using graphite monochromated MoKα (λ = 0.71073 Å) radiation in a Bruker APEX II diffractometer. The structure was solved by direct methods, and full-matrix least-squares refinement of the structural model was performed. All non-hydrogen atoms were refined anisotropically. Hydrogen atoms were placed at calculated idealized positions and refined as riding using SHELXL-2018/1 default values [27], except for those of the N−H and O−H groups that where refined isotropically with a displacement parameter constrained to 1.2x and 1.5x of their parent atoms, respectively. The occupancy of the disordered carboxylic atom (see below) was fixed at 0.5. Full details on data collection and structure refinement are provided in the Supporting Information (SI). A summary of the data collection and refinement details is given in Table 1. A CIF file containing the supplementary crystallographic data was deposited at the Cambridge Crystallographic Data Centre, with reference CCDC 1996470.

All calculations were undertaken for the isolated species in the vacuum using Gaussian 09 [28], with the B3LYP functional and the 6-311++G(d,p) basis set [29-32]. The calculated vibrational frequencies were scaled by 0.918, 0.971 and 1.023 (above 3400 cm^{-1}, between 3400 and 1600 cm^{-1}, and below 1600 cm^{-1}, respectively) which were chosen in order to obtain a better description of the observed spectra by the theoretical data. The calculated vibrational modes were approximately characterized by using the animation module of ChemCraft [33].

Table 1 – Summary of the single-crystal X-ray data collection and crystal structure refinement.

Chemical formula	$C_{10}H_{11}N_4NaO_8$
Color, shape	Clear colorless, block
Formula weight	338.22
Space group	$P2_1/n$
Temperature(K)	293(2)
Crystal system	monoclinic
a (Å)	7.9613(14)
b (Å)	10.4664(19)
c (Å)	8.1592(14)
α (deg)	90
β (deg)	94.491(6)
ɣ (deg)	90
Cell volume (Å ^{3})	677.8(2)
Z	2
D_c (Mg m^{-3})	1.657
Diffractometer/scan	Bruker ApexII/ ϕ and *ω* scans
Radiation (Å) (graph. monochromated)	0.71073
Max. crystal dimensions (mm)	0.13×0.11×0.06
Θ range (deg)	3.221-24.993
Range of *h, k, l*	–9,9; –12,12; –9;9
Reflections measured/independent	7800/1192
Reflections observed ($I > 2\ \sigma$)	696
Corrections applied	Absorption (Multi-scan, SADABS)
Computer programs	APEXIII, SHELXT-2014/5, SHELXL-2018/1, PLATON, VESTA
Structure solution	Direct Methods
Data/restraints/parameters	1192/0/115
GOF	1.025
R_1 ($I > 2\ \sigma$)	0.0457
wR_2	0.1076
Function minimized	$\Sigma\ w\ (\lvert F_o\rvert^2 - S\lvert F_c\rvert^2)$
Diff. density final max/min (*e* Å^{-3})	0.226, –0.284

Results and Discussion

In our previous study on 5AAH [24] we have shown that the compound crystallizes in the $P2_12_12_1$ space group, with one molecule in the asymmetric unit, which assumes the conformation of the highest energy conformer predicted for the isolated molecule (see Fig. 1). As mentioned in the introduction, the fact that the selected conformer (*trans*-III) upon crystallization of the compound (polymorph I, most stable polymorph at room temperature) is the highest energy conformer among 13 conformers of the molecule, with an energy ~40 kJ mol^{-1} above that of the most stable conformer (*cis*-I; see Fig. 1) is unique. In the 5AAH crystal, 3 different types of hydrogen bonds are present. Taken a

molecule as reference, the first, connects the OH group of the acetic acid substituent of the molecule to the oxygen atom of the ring carbonyl group of a neighbour molecule which is vicinal to two NH groups (O–H···O= type H-bond, with d(O···O) = 2.615 Å and <(O–H···O) = 166°); the second, connects the N–H group of the ring that stays between the two carbonyl groups of the hydantoin ring of the considered molecule to the oxygen atom of the second ring carbonyl group of another neighbour molecule (N–H···O= type H-bond, with d(N···O) = 2.836 Å and <(N–H···O) = 166°); and the third, connects the second N–H group of the molecule to the acid oxygen atom of a third neighbour molecule (N–H···O= type H-bond, with d(N···O) = 3.010 Å and <(N–H···O) = 175°). The H-bond acceptor moieties of the molecule receive H-bonds of these 3 types where the donors belong to neighbour molecules. A particularly interesting structural peculiarity is that the carbonyl oxygen atom of the acetic acid substituent is not involved in any classical H-bond in the crystal of 5AAH (instead, it participates in two non-classical CH···O interactions with two neighbour molecules). As it will be shown below, this pattern of hydrogen bonding is completely different from that existing in the sodium salt of the compound. Also, the conformation assumed by the 5AAH hydantoin molecules in the crystal of the salt is not the same as in the neat 5AAH crystal described above. Such facts prove the structural/conformational versatility of the 5AAH molecule.

Single Crystal X-Ray Diffraction Analysis of the Sodium Salt of 5AAH

The compound crystallizes in the $P2_1/n$ monoclinic space group with unit cell parameters a = 7.9613(14) Å, b = 10.4664(19) Å, c = 8.1592(14) Å, β = 94.491(6)°. The structure is a 3D coordination polymer built around the metal ions which are hexa-coordinated with oxygen atoms from the organic moiety in a pseudo-octahedral geometry (Fig. 2).

The Na atoms sit on inversion centers at the special positions ½, ½, 0; 0, 0, ½ (Wyckoff site: *b*) with multiplicity 2, whereas the atoms of the organic moiety sit at general positions of multiplicity 4. This means that the ratio between the number of Na atoms and the organic moiety is fixed by the crystallographic space group as 1:2, thus corresponding to the chemical formula $C_{10}H_{11}N_4NaO_8$ (or $Na(5AAH)_2$). Therefore, charge neutrality can only be achieved if one out of two organic moieties is single charged, meaning an average anionic charge per organic moiety of −0.5 *e*.

The coordination geometry is determined out of any doubt and is described in details below, but it is clear that the NH moieties of the hydantoin ring are protonated and do not

participate in the coordination with the metal. In this regard, the coordination of 5AAH in the studied complex does not follow the general trend of hydantoins, which usually bound *via* the deprotonated NH group of the ring which is vicinal to the two carbonyl groups (N3-H in Fig. 2) (see the illustrative example described in Ref. [26]). Coordination through the deprotonated carboxylic moiety of 5AAH, with the two NH groups of the ring being protonated, has been reported for the tetra-aqua-bis-5AAH Co^{II} complex [34], showing that the most labile group to deprotonation in 5AAH is indeed the carboxylic moiety thus favoring complexation of the molecule where the structural integrity of the hydantoin ring is preserved.

In the studied substance, the found structural formula, together with the observation that the hydantoin ring keeps its structural integrity, implies that the carboxylic group is on average half deprotonated. Indeed, the H atom of the carboxylic O16 atom (see Fig. 2) was found to be disordered and in a *trans* position while being involved in a hydrogen bond with the same atom of a neighbour symmetry related molecule (Fig. 3). Thus, a single H atom is shared by the two molecules, with 50% probability of acting as an acceptor/donor.

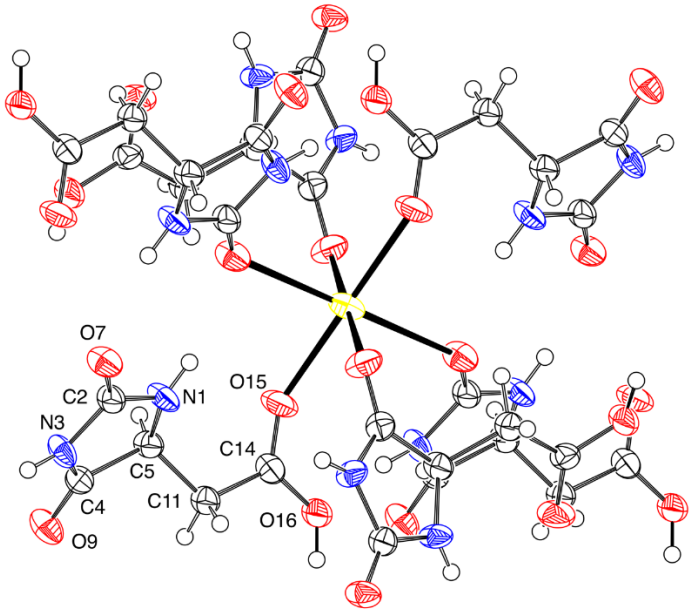

Figure 2. ORTEP plot of the cation coordination shell showing the anisotropic displacement ellipsoids drawn at the 50% probability level.

The measured O16···O16 distance of 2.453(5) Å is indeed characteristic of a strong hydrogen bond. The disordered H atom was included in the refinement with a fixed occupancy of 0.5, therefore describing the average structure in what concerns this particular hydrogen bond. Whether the proton is truly randomly disordered corresponding to the average structure

described in the $P2_1/n$ space group or rather fully or partially ordered (implying a lower symmetry space group) cannot be disclosed from our XRD data. However, refinement on $P2_1/n$ converged to a low *R*-factor, with no anomalies found upon examination of the anisotropic displacement ellipsoids of the non-H atoms. Therefore, any putative distortion of the structure due to ordering of the shared carboxylic H atom would be very small. Moreover, tentative refinements on lower symmetry space groups allowing two-inequivalent organic moieties (one neutral, the other deprotonated) could not refine properly because of the strong correlation between the structural parameters due to the pseudo-symmetry.

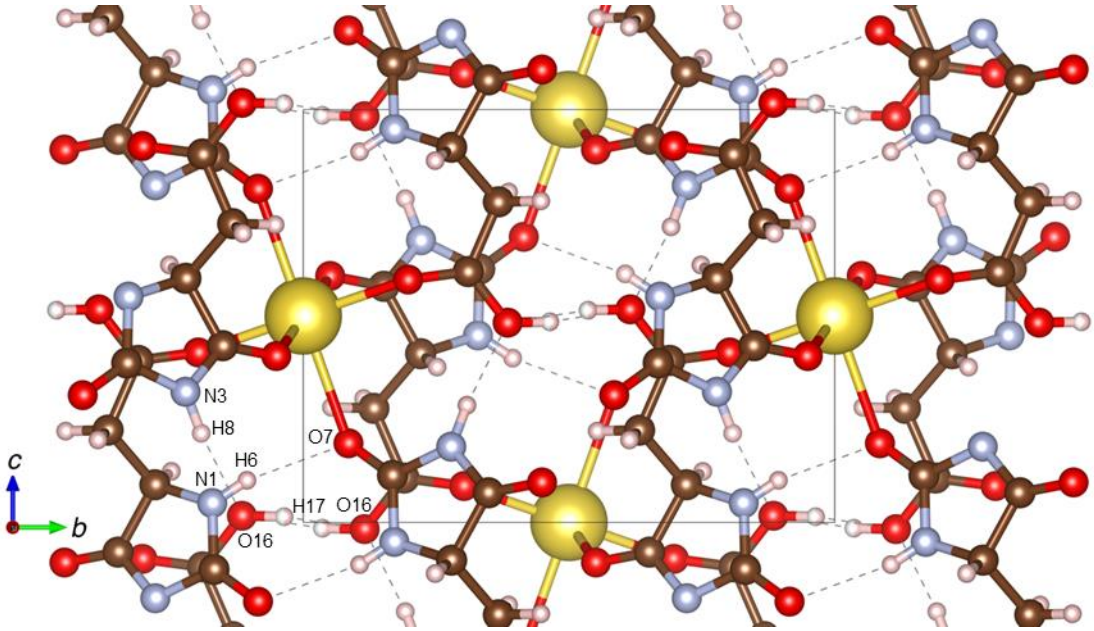

Figure 3. Projection of the crystal structure along the *a*-axis. Hydrogen bonds are depicted as dashed lines, the disordered hydrogen bond involving the carboxylic H atom is depicted as a double dashed line.

The Na ion sits on inversion centers, therefore the coordination polyhedron features only 3 distinct Na–O bonds, with bonding distances 2.291(2), 2.334(2) and 2.670(2) Å, the shortest one being that involving the carbonyl O15 atom of the ligand, and the second and third ones involving the ring O9 and O7 atoms, respectively. All carbonyl oxygen atoms of the 5AAH ligand are then involved in the coordination to the metal. The O–Na–O angles in the plane perpendicular to the longest Na–O bond are 87.7°/(92.3°). The angles in one of the two coordination planes containing the longest Na-O, 80.21(99.79), deviate more strongly from the ideal value (90°), while in the other plane they are close to the ideal value, 89.05/(90.05). The

distorted pseudo-octahedral volume is 18.729 Å^3, with a quadratic elongation of 1.020 and an angle variance of 37.08°^{2} [35]. The O atom involved in the longest Na–O bond (O7) also participates as an H-bond acceptor from one of the two NH groups of a neighbour molecule (N1-H) (Table 2). The other NH group (N3-H) of the hydantoin ring also participates in hydrogen bonding as a donor towards the O16 atom of the carboxylic group of another neighbour molecule.

Table 2 – Hydrogen bonds and short intermolecular contacts. Distances and angles are given in Å and degrees, respectively. Symmetry codes: a) 1–*x*,1–*y*,1–*z*; b) x,y,–1+*z*; c) 1–*x*,2–*y*,1–*z*; d) 1–*x*,2–*y*,2–*z*; *e*) *x*–1/2, –*y*+3/2, *z*–1/2.[a]

D-H···A	D-H	H-A	D···A	< D-H···A
N1–H6···O7[a]	0.82(3)	2.14(3)	2.937(4)	166(3)
N3–H8···O16[b]	0.90(3)	1.89(3)	2.784(3)	174(3)
O16–H17···O16[c]	0.87(8)	1.61(8)	2.454(3)	164(13)
C11–H12···O9[d]	0.97	2.46	3.304(4)	145
C5–H10···O16[e]	0.98	2.66	3.487(4)	142.7

[a] See Figure 3 for atom numbering.

Concerning the geometry of the 5AAH molecules in the crystal, the hydantoin ring has the expected planar geometry (r.m.s. deviation from the least-squares plane of 0.02 Å), the O9 atom lying in the plane whereas atom O7 is slightly out of the plane (0.11 Å). The weighted average torsion angle within the ring is 3.2(2)°. The least-squares plane of the substituent atoms forms an angle of 49.5(1)° with the ring plane. The relevant torsion angles O15=C14–C11–C5 and C14–C11–C5–C4 are 12.03° and 170.3°, respectively, which are very similar to those of conformer *trans*-**I** (see Fig. 1) found for the isolated molecule of 5AAH, 2.89° and 171.4°, respectively [24]. According to the DFT(B3LYP)/6-311++G(d,p) calculations reported in Ref. [24], conformer *trans*-**I** is the second most stable form of 5AAH bearing the carboxylic group in the *trans* geometry (O=C–O–H dihedral of *ca.* 180°), with a relative energy to the ground conformational state (*cis*-**I**; see Fig. 1) of 22.9 kJ mol^{-1}. Though it is considerable more stable than the conformer present in the crystal of the neat hydantoin (form *trans*-**III**, with a relative energy of 39.3 kJ mol^{-1} [24]), conformer *trans*-**I** is still a high-energy conformer of 5AAH (8th out of 13 conformers in order of energy). This result reinforces the conclusion that 5AAH is a structurally very versatile molecule, which is able to participate in strong intermolecular interactions that can supersede the intrinsic higher structural stability of the individual molecules and lead to selection of higher energy conformers on formation of a crystalline phase.

Raman spectra of the Sodium Salt of 5AAH

Figures 4 and 5 show the Raman spectrum of the $Na(5AAH)_2$ compound, together with that of the neat 5AAH (polymorph I), in the high and low frequency regions, respectively. These spectra are compared with those simulated based on the DFT(B3LYP)/6-311++G(d,p) calculated Raman spectrum for the isolated-molecule 5AAH conformer *trans*-**III** (which is the constituting unit of the neat 5AAH crystal) and for the 1:1 cationic $[Na\text{-}5AAH]^+$ species where the 5AAH molecule was kept fully protonated and in the *trans*-**I** conformation (as found in the crystal of the salt by XRD). Several other models were used to help interpretation or simulate the Raman spectrum of the crystalline salt (see Figs. S1 and S2 in the SI, where the corresponding DFT(B3LYP)/6-311++G(d,p) calculated Raman spectra are shown): (i) the 5AAH isolated-molecule *trans*-**I** conformer (the conformer of 5AAH existing in the crystal of the salt as determined by XRD), (ii) the 1:1 neutral Na-5AAH complex, where the 5AAH molecule has its carboxylic group deprotonated, and (iii) the 2:2 cationic $[Na_2\text{-}5AAH_2]^+$ species represented in Fig. S3 in the SI, where an O···H···O bond established between two molecules of the hydantoin is present (this structure was made centrosymmetric in an attempt to mimic the relevant structural unit of the crystal, and the minimum number of Na ions were included – bound to the O15 atoms which were found to form the strongest coordination bond –, in order to keep the model as simple as possible).

The Raman spectrum of the neat hydantoin crystal is reasonably described by the calculated Raman spectrum of isolated conformer *trans*-**III**, in particular in the high frequency region (including the carbonyl stretching region) and below ca. 1000 cm^{-1}. Naturally, those vibrations that are expected to be more sensitive to intermolecular interactions, *e.g.*, OH and NH stretching modes, cannot be duly described by such a simple model, but the observed shifts between the calculated and observed bands can also be used to shed light on structural characteristics of the system, as pointed out below. In turn, the Raman spectrum of the $Na(5AAH)_2$ crystal is not properly described at all by the calculated spectrum of the isolated 5AAH *trans*-**I** conformer, nor by the 1:1 neutral Na-5AAH complex where the 5AAH molecule has its carboxylic group deprotonated (see Figs. S1 and S2 in the SI). Besides intermolecular interactions, in the first case complexation is not accounted for, while in the second case the presence of a hydrogen atom connected to O16 is not taken into account. On the other hand, the calculated spectrum for the 1:1 cationic $[Na\text{-}5AAH]^+$ species, where the 5AAH molecule was kept fully protonated and in the *trans*-**I** conformation, describes quite reasonably some of

the most relevant features observed in the experimental spectra of the compound. This unequivocally demonstrates the relevance of the presence of a hydrogen atom bound to the carboxylic group of the 5AAH molecules in the crystal also in determining the vibrational spectra of the compound. Somehow unexpectedly, the spectrum calculated for the more complex 2:2 cationic $[Na_2\text{-}5AAH_2]^+$ system (Figs. S1 and S2 in the SI) shows a worse agreement with the experimental spectrum of the 5AAH sodium salt than that obtained using the 1:1 cationic $[Na\text{-}5AAH]^+$ model, so that in this latter will be used in the discussion below.

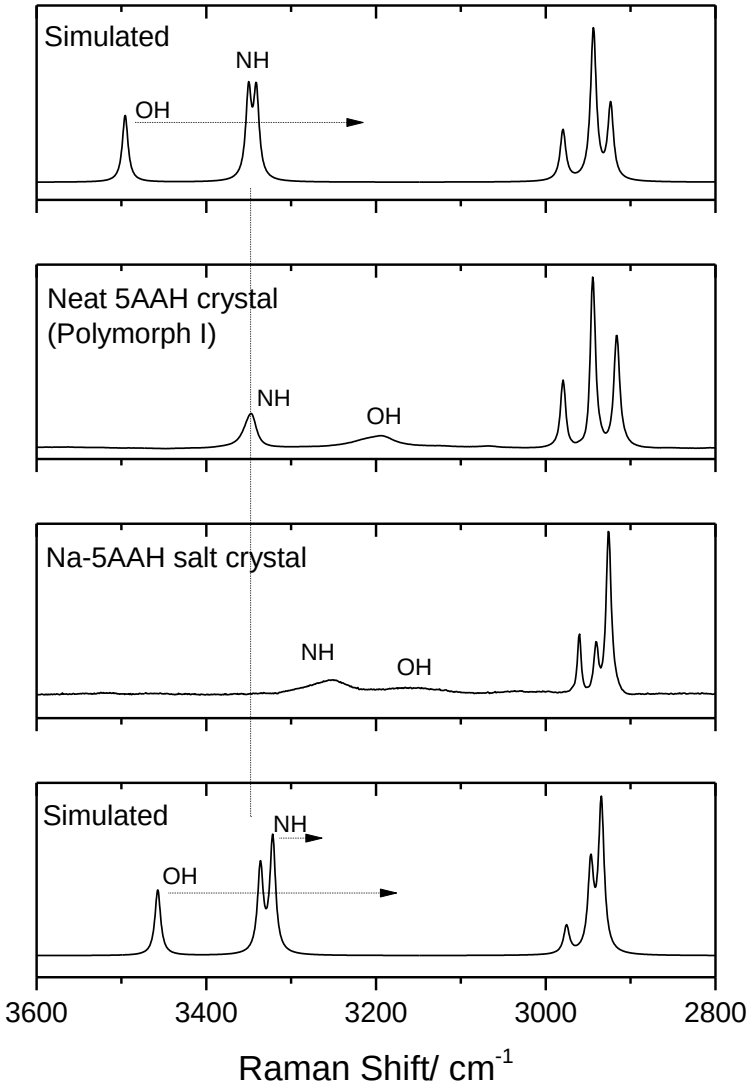

Figure 4. High frequency region of the room temperature experimental Raman spectra of the neat crystal of 5AAH (polymorph I) and of the synthesized sodium salt of the hydantoin [mid spectra], and DFT(B3LYP)/6-311++G(d,p) calculated Raman spectra for *trans*-**III** conformer of 5AAH and the 1:1 cationic $[Na\text{-}5AAH]^+$ species where the 5AAH molecule was kept fully protonated [top and bottom spectra]. In the calculated spectra, frequencies were scaled as described in the section Experimental Procedures and Computational Methods, and the intensities were obtained by dividing the calculated Raman activity of each mode (expressed in in $Å^4\,(AMU)^{-1}$) by its frequency (Raman shift expressed in cm^{-1}). The arrows indicate the shifts due to intramolecular hydrogen bonding taken as reference the calculated scaled values of the used models. The vertical dashed line is only to guide the eyes for better comparison between the positions of the bands ascribed to the NH stretching modes.

In the high frequency spectral region, the spectral profiles of the experimental Raman spectra of the 5AAH and its sodium salt, as well as the changes in going from one system to the other, are very well reproduced by the calculated spectra for the isolated 5AAH *trans*-**I** conformer and 1:1 cationic $[Na\text{-}5AAH]^+$ species in what concerns the C-H stretching vibrations (the group of intense bands around 3000 cm^{-1}). The relative positions of the bands ascribable to the NH stretching modes are also predicted properly by the two simple molecular models. After scaling, the calculated values are 3350/3341 cm^{-1} (5AAH) and 3336/3322 cm^{-1} ($[Na\text{-}5AAH]^+$). The scale factor in this spectral region was chosen to allow reproduction of the experimental value for the NH stretching modes in the neat crystal of 5AAH (3347 cm^{-1}), so that the matching between the experimental and calculated values for this system was imposed by the used scaling criterion. However, this criterion was used because it allows to get some information regarding the relative strength of the intermolecular H-bond interactions involving the NH groups in the two crystals. Indeed, the fact that the experimentally observed NH stretching bands in the experimental spectrum of the crystalline salt (3289/3255 cm^{-1}) are shifted to lower frequencies in comparison with the calculated values for the used model indicate that the H-bonds involving the NH groups in the crystal of the sodium salt of 5AAH are stronger than those in the crystal of the neat compound. This is in agreement with the structural data presented in the previous section, as detailed below. In turn, the bands due to the OH stretching vibrations in the experimental spectra are observed at much lower values in both chemical systems (major bands at 3194 and *ca.* 3150 cm^{-1}, for 5AAH and its sodium salt, respectively) than those predicted theoretically and scaled by the same scale factor used for the NH stretching modes, which clearly correlates with the fact that the intermolecular H-bond interactions in the crystals involving the OH moiety as donor are the strongest ones in both crystals. Comparing the frequencies for both NH and OH stretching modes in the two crystals one can see that they are observed at lower frequencies in the salt, which is in consonance with the presence of stronger H-bond interactions in the last crystalline material and agrees with the structural information obtained from XRD (O16···O16, N1···O16 and O1···O17 H-bond distances in the salt are 2.454, 2.784 and 2937 Å, respectively, while the related H-bond distances in the neat 5AAH crystal are 2.615, 2.836 and 3.010 Å [24]). The relative broadness of the bands ascribed to the NH and OH stretching modes in the two crystals are also in agreement with stronger H-bonds in the salt (broader bands) than in neat 5AAH (less broad bands).

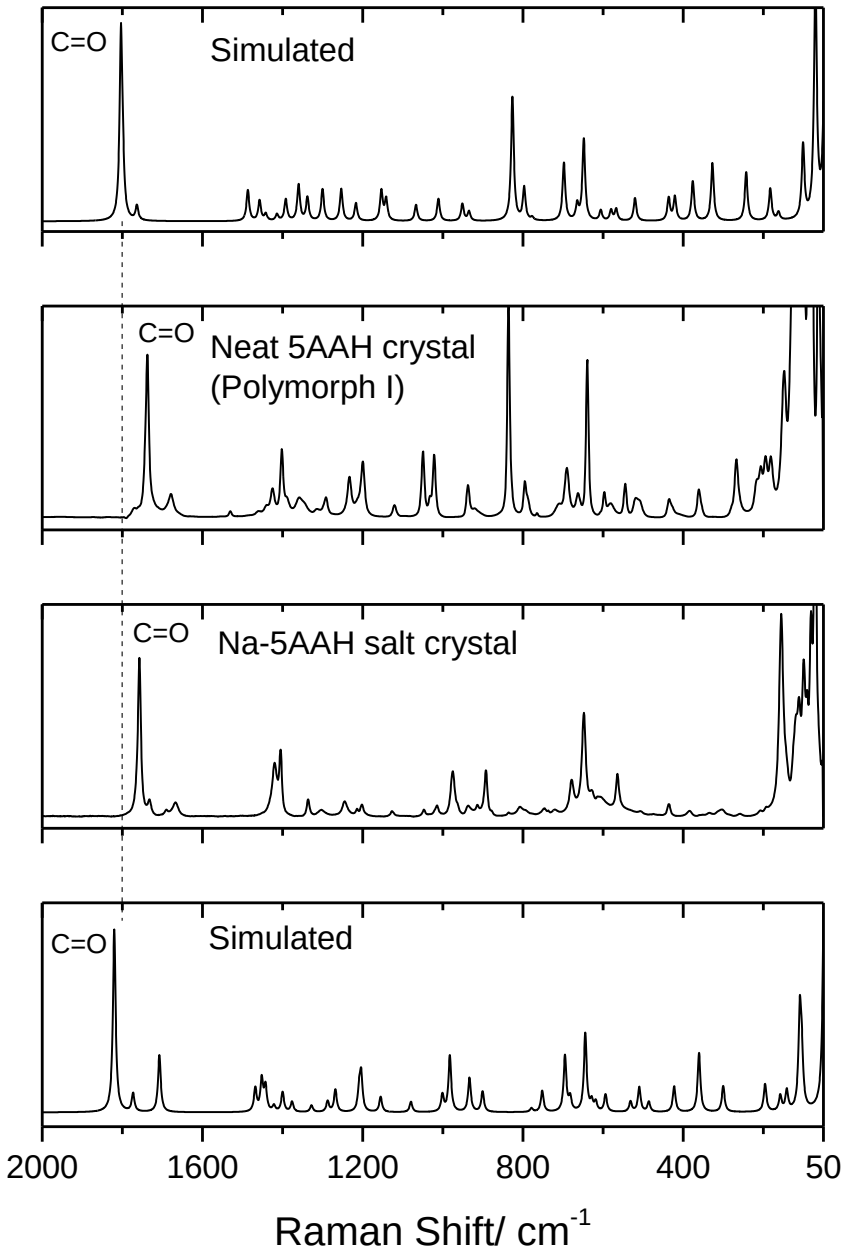

Figure 5. Low frequency region of the room temperature experimental Raman spectra of the neat crystal of 5AAH (polymorph I) and of the synthesized sodium salt of the hydantoin [mid spectra], and DFT(B3LYP)/6-311++G(d,p) calculated Raman spectra for *trans*-III conformer of 5AAH and the 1:1 cationic $[Na\text{-}5AAH]^+$ species where the 5AAH molecule was kept fully protonated [top and bottom spectra]. In the calculated spectra, frequencies were scaled as described in the section Experimental Procedures and Computational Methods, and the intensities were obtained by dividing the calculated Raman activity of each mode (expressed in in $Å^4\,(AMU)^{-1}$) by its frequency (Raman shift expressed in cm^{-1}). The vertical dashed line is only to guide the eyes for better comparison between the positions of the bands ascribed to the C=O stretching modes.

In the carbonyl stretching spectral region, the calculated frequencies (frequencies scaled using the same scale factor as for the CH stretching modes, which are not particularly sensitive to intermolecular interactions) considerably overestimate the observed frequencies, which is consistent with the involvement of the carbonyl groups in H-bonding interactions in the

crystalline materials. The observation of the band at 1691/1668 cm^{-1} in the spectrum of the salt, which is assigned to the stretching mode of the carbonyl moiety of the acetic acid substituent, clearly reveals the involvement of this moiety in the coordination with the metal (in the spectrum of the neat 5AAH crystal the band due to this vibration is buried within the intense vibration at 1738 cm^{-1}). On the other hand, the two bands ascribed to the ring carbonyl stretching vibrations (better described as symmetric and anti-symmetric vibrations involving the two carbonyl groups, according to the calculations) are observed to occur at higher frequency in the salt. This trends shall essentially be due to indirect effects of the binding to the sodium ion since, on one side, the opposite order of frequencies is observed when the calculated spectra of the *trans*-**III** 5AAH conformer (existing in the neat 5AAH crystal) and *trans*-**I** conformer (existing in the salt) are compared and, on the other side, the same order of frequencies is observed in the calculated spectra of the *trans*-**III** 5AAH conformer and of the $[Na\text{-}5AAH]^+$ species.

Other vibrational mode that could be expected to be very much sensitive to H-bonding is the OH torsion, while the vibrations having major contributions of the C-O stretching and COH bending coordinates (that usually mix extensively) could also be expected to be influenced by the H-bonding in some extent [36-38]. The OH torsion in 5AAH is ascribable to the band observed at 518 cm^{-1}, which are considerably blue shifted compared to the predicted position for the isolated molecule (436 cm^{-1}) as expected for a strong hydrogen bonded group [38]. In the spectrum of the salt, the torsional vibration shall appear at an even considerably higher frequency, since the H bond in which the OH group is involved is stronger than in the neat crystalline 5AAH, and most probably contributes to the intensity of the broad spectral feature observed at *ca.* 609 cm^{-1}. The pairs of bands due to the mixed C-O stretching/COH bending coordinates are predicted by the used simple models at 1300 and 1153 cm^{-1} (5AAH) and 1327 and 1203 cm^{-1} ($[Na\text{-}5AAH]^+$), and assigned to the pairs of bands at 1292 and 1121 cm^{-1} and 1303 and 1127 cm^{-1}, respectively, being slightly higher in frequency for the salt, as expected considering the stronger H-bond involving the OH group in this crystal.

The most intense Raman bands appearing in the low frequency range in the experimental spectra (above 200 cm^{-1}) are observed at 836 and 640 cm^{-1}, in the case of the crystal of 5AAH, and at 974 and 649 cm^{-1} for the 5AAH sodium salt. The higher frequency bands has a large contribution from the stretching mode of the C–C bond alfa to the carboxylic moiety, while the lower frequency band corresponds to a hydantoin ring deformational mode. These modes are

predicted at 826 and 648 cm^{-1} for the *trans*-III 5AAH conformer and at 982 and 644 cm^{-1} for the $[Na\text{-}5AAH]^+$ species, in good agreement with the experimental data and demonstrating that these vibrations are not particularly sensitive to the intermolecular environment.

A general tentative assignment of the Raman spectra of the two crystalline materials is provided in Table 3, together with the calculated frequencies and Raman activities for the chosen model systems.

Conclusion

Following our interest on the structure, reactivity, thermal and spectroscopic properties of hydantoins [19-24], in particular our recent investigation of 5AAH, which was found to exhibit the rather unusual structural behaviour of selecting, as structural units for the most stable room temperature crystalline phase, the highest-energy conformer among 13 possible conformers of the molecule [24] (with an energy higher by ~40 kJ mol^{-1} than that of the conformational ground state), in the present study we have investigated the sodium salt of the compound. Our main interest was to find if the peculiar structural behaviour of 5AAH would also manifest in the properties of the salt.

As shown above, the salt revealed itself a very interesting, from the structural point of view, crystalline material, and also confirmed the structural versatility of 5AAH. This was shown directly through the determination, by XRD, of the structure of the crystal of the newly synthesized salt, but also indirectly by Raman spectroscopy, supported by DFT calculations of the Raman spectra of simple models of the crystals of both the salt and the neat hydantoin, built based on their relevant structural elements.

First of all, the 5AAH molecules in the crystal give rise to a pseudo-octahedral coordinating geometry and bind *via* their oxygen atoms, instead of *via* a deprotonated ring nitrogen as is commonly found for hydantoins [26]. The lability of the carboxylic hydrogen atom of the acetic acid substituent justifies the preference of coordination *via* the carboxylic group, and also determines the very interesting formal charge of the hydantoin in the crystal, which is −0.5 *e*. DFT(B3LYP)/6-311++G(d,p) calculations performed in this study on the simple 1:1 Na-5AAH complexes where the carboxylic group or the most acidic hydantoin ring nitrogen atom (N3) are deprotonated showed that the first complex is more stable than the second by 62.2 kJ mol^{-1}, in agreement with the observations.

Table 3. Assignment of the Raman spectra of 5AAH (polymorph I) and of the sodium salt of the hydantoin, and DFT(B3LYP)/6-311++G(d, p) calculated data for the isolated trans-III conformer of 5AAH and the $[Na\text{-}5AAH]^+$ and $[Na_2\text{-}5AAH_2]^+$ species. [a]

5AAH (Polymorph I) Exp. Freq.	5AAH *trans*-III Calc. Freq.	Raman activity	Na-5AAH Crystal Exp. Freq.	$[Na\text{-}5AAH]^+$ Calc. Freq.	Raman activity	Assignment[b]
3347	3350/3341	103.0/101.7	3289/3255	3336/3322	84.2/111.6	$\nu(N_1H)$, $\nu(N_3H)$
3194/3066	3496	82.8	3150/3033	3457	66.0	ν(OH)
2980	**2980**	**53.7**	2961	**2976**	**24.2**	$\nu(CH_2)_{as}$
2945	**2944**	**158.6**	2926	**2935**	**128.9**	$\nu(CH_2)_s$
2916	**2924**	**77.7**	2940	**2947**	**74.3**	ν(CH)
1770/1738	**1803**	**40.9**	1758	**1820**	**43.9**	$\nu(C{=}O)_s$
1738	**1799**	**7.7**	1691/1668	**1708**	**12.9**	$\nu(C_{14}{=}O)$
1679	**1764**	**3.2**	1734	**1773**	**4.3**	$\nu(C{=}O)_{as}$
1460	**1487**	**5.7**	1420	**1468**	**4.5**	$\delta(CH_2)$
1439/1425	**1458**	**3.7**	1404	**1452**	**6.1**	$\delta(N_1H)$
1402	**1442**	**1.2**	1404	**1443**	**4.7**	γ(CH)
1402	**1414**	**1.1**	n.obs.	**1422**	**1.1**	$w(CH_2)$
1358	**1392**	**3.7**	1336	**1400**	**3.6**	$\delta(N_3H)$
1346	**1360**	**6.1**	1312	**1376**	**1.8**	ν_3(ring)
1314	**1338**	**3.8**	1246	**1288**	**1.8**	ν_2(ring)
1292	**1300**	**5.1**	1303	**1327**	**1.2**	δ(COH)
1233	**1254**	**5.0**	1214	**1268**	**3.8**	$tw(CH_2)$
1200	**1217**	**2.7**	1202	**1209**	**3.2**	ν_1(ring)
1121	**1153**	**4.3**	1127	**1203**	**5.8**	$\nu(C_{14}\text{-}O)$
1049	**1142**	**3.0**	1046	**1155**	**2.3**	$\nu(C_5\text{-}C_{11})$
1032	**1067**	**2.1**	1023	**1080**	**1.5**	$\gamma(CH_2)$
1022	**1011**	**2.8**	1015	**1001**	**2.2**	ν_5(ring)
937	**951**	**2.0**	937	**934**	**4.2**	γ(CH)
921/912	**935**	**1.1**	913/893	901	2.4	ν_4(ring)
836	**826**	**12.7**	974	**982**	**7.3**	$\nu(C_{11}\text{-}C_{14})$
795/789	**797**	**3.2**	836/807	**779**	**0.4**	$\gamma(C_2{=}O)$
765	**777**	**0.3**	745/722	**752**	**2.1**	δ_2(ring)
709/690	**698**	**5.0**	675	**695**	**5.1**	$\gamma(C_4{=}O)$
663	**665**	**1.3**	675	**682**	**1.2**	$\gamma(C_{14}{=}O)$
640	**648**	**6.6**	649	**644**	**6.7**	δ_1(ring)
597	**606**	**0.8**	631	**628**	**0.8**	$\gamma(N_3H)$
582	**580**	**0.8**	614	**618**	**0.8**	δ(CC=O)
545	**567**	**0.8**	609	**594**	**1.4**	$\delta(C_2{=}O)$, $\delta(C_4{=}O)$
518	**436**	**1.2**	609	**532**	**0.7**	τ(OH)
509	**520**	**1.5**	566	**510**	**1.7**	$\gamma(N_1H)$
435	**421**	**1.2**	n.obs.	**486**	**0.6**	δ(CCO)
361	**376**	**1.8**	430	**423**	**1.4**	$\delta(C_{11}$(ring))
278/267	**327**	**2.3**	385	**361**	**2.8**	$\delta(C_2{=}O)$, $\delta(C_4{=}O)$
215/206	**243**	**1.5**	334	**300**	**1.0**	$\gamma(C_{11}$(ring))
195/181	**183**	**0.7**	252/208	**196**	**0.7**	τ_2(ring)
148	**162**	**0.2**	199	**158**	**0.3**	δ(CCC)
124/111	-	-	153/117/111	-	-	Intermolecular
88	101	0.9	99/92	**109**	**1.4**	τ_1(ring)
79	**70**	**2.1**	80	**104**	**0.7**	$\tau(C_5\text{-}C_{11})$
63	**44**	**2.0**	71	**49**	**1.4**	$\tau(C_{11}\text{-}C_{14})$

[a] Number in parentheses are Raman activities in $Å^4\,(AMU)^{-1}$. Note that the intensities used to simulate the theoretically calculated spectra shown in Figs. 4 and 5 were obtained by dividing the Raman activity of each mode by its frequency (Raman shift) and multiplying the result by 100. Calculated frequencies were scaled by 0.918, 0.971 and 1.023 (above 3400 cm^{-1}, between 3400 and 1600 cm^{-1}, and below 1600 cm^{-1}, respectively). For the $[Na\text{-}5AAH]^+$ model, the vibrational modes involving the Na atom are not included in the table, they were calculated at 24, 31 and 104 cm^{-1} (scaled values). [b] Numbering of atoms as in Fig. 2. Abbreviations: s, symmetric; as, anti-symmetric; ν, stretching; δ, in-plane bending; γ, out-of-plane bending; τ, torsion, w, wagging; tw, twisting. Approximate description of vibrations was obtained by visual inspection of modes using the animation module of Chemcraft [33].

Additionally, the conformation adopted by the 5AAH molecules in the crystal of its sodium salt (*trans*-I) was determined to be different both from that existing in the gas phase of the hydantoin (the most stable conformer for the isolated matrix: *cis*-I [24]) and from the one present in the neat crystalline compound (most stable polymorph at room temperature): *trans*-III. Interestingly, the conformer existing in the crystal of the salt resembles more that existing in the gas phase of the 5AAH, than that found in the crystal of the neat compound whose structure has already been solved (polymorph I [24]) (see Fig 1). Indeed, conformer *trans*-I (present in the salt) differs from the most stable 5AAH conformer found in gas phase of the hydantoin only by changing the conformation within the carboxylic group (from *cis* to *trans*, as it can be observed in Fig 1), while conformer *trans*-III (present in the neat crystalline 5AAH polymorph I) differs from the conformational ground state both in the conformation within the carboxylic group and in the relative orientation of the whole acetic acid substituent in relation to the hydantoin ring.

This is the first comprehensive investigation on the crystal properties of the sodium salt of 5AAH, and the obtained data, together with previously reported information on the molecular properties of hydantoins and on the properties of simple hydantoins in the crystalline state [19-24], will certainly constitute a source of fundamental structural and spectroscopic information for those working on applications of hydantoins, in particular for those interesting to address its mechanisms of action at a molecular level, which can be expected to be mostly determined by characteristic structural aspects of the compounds.

Supporting Information

Figures S1 and S2, with the Raman spectra of 5AAH neat crystal and crystalline 5AAH sodium salt and DFT(B3LYP)/6-311++G(d,p) calculated spectra for model systems in the high and low frequency regions, respectively; Figure S3, with the DFT(B3LYP)/6-311++G(d,p) optimized structure of the cationic 2:2 $[Na2\text{-}5AAH2]^{+}$ species. Tables S1-S9 with the crystallographic data. This data is available free from internet from http://...

Acknowledgements

The authors acknowledge financial support from the Portuguese Science Foundation ("Fundação para a Ciência e a Tecnologia" - FCT) – Projects CQC UIDB/00313/2020 and

UIDP/00313/2020, also co-funded by FEDER/COMPETE 2020-EU. CFisUC is funded by FCT through the projects UIDB/04564/2020 and UIDP/04564/2020. Access to instruments from Laser-Lab Coimbra and TAIL-UC facilities funded under QREN-Mais Centro is gratefully acknowledged. B.A.N. also acknowledges FCT for the SFRH/BD/129852/2017 PhD Scholarship.

References

1. U.K. Department of Health, *British Pharmacopeia Online*; 2011, Vols. I and II, Monograph 1207.
2. M. J. Finkel, Phenytoin Revisited. *Clin. Ther.* 1984, 6, 577–591.
3. J. H. Fischer, T. V. Patel and P. A. Fischer, Fosphenytoin: Clinical Pharmacokinetics and Comparative Advantages in the Acute Treatment of Seizures. *Clin. Pharmacokinet.* 2003, 42, 33–58.
4. C. F. Thorn, M. Whirl-Carrillo, J.S. Leeder, T. E. Klein and R. B. Altman, PharmGKB Summary: Phenytoin Pathway. *Pharmacogenet Genomics.* 2012, 22, 466–470.
5. T. Krause, M. U. Gerbershagen, M. Fiege, R. Weisshorn and F. Wappler, Dantrolene: A Review of its Pharmacology, Therapeutic Use and New Developments. *Anaesthesia* 2004, 59, 364–73.
6. K. Paul-Pletzer, T. Yamamoto, M. B. Bhat, J. Ma, N. Ikemoto, L. S. Jimenez, H. Morimoto, P. G. Williams and J. Parness, Identification of a Dantrolene-binding Sequence on the Skeletal Muscle Ryanodine Receptor. *J. Biol. Chem.* 2002, 277, 34918–34923.
7. A. Elizalde and J. Sanchéz-Chapula, Effects of the Novel Antiarrhythmic Compound TR 2985 (Ropitoin) on Action Potentials of Different Mammalian Cardiac Tissues, *Naunyn-Schmiedeberg's Arch. Pharmacol.* 1988, 37, 316–322.
8. C. S. A. Kumar, C. V. Kavitha, K. Vinaya, S. B. B. Prasad, N. R. Thimmegowda, S. Chandrappa, S. C. Raghavan and K. S. Rangappa, Synthesis and in Vitro Cytotoxic Evaluation of Novel Diazaspiro Bicyclo Hydantoin Derivatives in Human Leukemia Cells: A SAR Study. Invest New Drugs. 2009, 27, 327–337.
9. C. V. Kavitha, M. Nambiar, C. S. A. Kumar, B. Choudhary, K. Muniyappa, K. S. Rangappa and S. C. Raghavan, Novel Derivatives of Spirohydantoin Induce Growth Inhibition Followed by Apoptosis in Leukemia Cells. *Biochem. Pharmacol.* 2009, 77, 348–363.
10. K. Yang, Y. Tang and K. A. Iczkowski, Phenyl-methylene Hydantoins Alter CD44-Specific Ligand Binding of Benign and Malignant Prostate Cells and Suppress CD44 Isoform Expression. *Am. J. Transl. Res.* 2010, 2, 88–94.
11. R. N. Comber, R. C. Reynolds, J. D. Friedrich, R. A. Manguikian, R. W. Buckheit, J. W. Truss, W. M. Shannon and J. A. Secrist, 5,5-Disubstituted Hydantoins: Syntheses and Anti-HIV Activity. *J. Med. Chem.* 1992, 35, 3567–3572.
12. V. G. Ovchinnikov and O. V. Gudz', The Antimicrobial Properties and Use of Sulfochloranthine (A Review of the Literature), *Vrach Delo* 1990, 2, 108–113.
13. F. Fang. C. Bernigaud, K. Candy, E. Melloul, A. Izri, R. Durand, F. Botterel, O. Chosidow, W. Huang and J. Guillot, Efficacy Assessment of Biocides or Repellents for the Control of Sarcoptes Scabiei in the Environment. *Parasit Vectors* 2015, 8, Art. 416.
14. European Food Safety Authority (EFSA), Peer Review of the Pesticide Risk Assessment of the Active Substance Iprodione, *EFSA Journal* 2016, 24, 1–31.
15. K. Drauz, I. Grayson, A. Kleemann, H.-P. Krimmer, W. Leuchtenberger and C. Weckbecker, Amino Acids. *Ullmann's Encyclopedia of Industrial Chemistry*, Willey 2007.

16. S. Deepa, B. Sivasankar, K. Jayaraman, K. Prabhakaran, S. George, P. Palani, K. S. Ramesh, C. V. Srinivasan, N. R. Kandasamy and A. K. Sadhukhan, Enzymatic Production and Isolation of D-Amino Acids from the Corresponding 5-Substituted Hydantoins, *Proc. Biochem.* 1883, 28, 447–452.
17. M. Miura, H. Masami, J. Kakizawa, A. Morita, T. Uetani and K. Yamada, Inhibitory Effect of L-Asparaginase in Lymphocyte Transformation Induced by Phytohemagglutinin. *Cancer Res.* 1970, 30, 768–772.
18. S. M. Sondhi, J. Singh, A. Kumar, H. Jamal and P. P. Gupta, Synthesis of Amidine and Amide Derivatives and Their Evaluation for Anti-Inflammatory and Analgesic Activities. *Eur. J. Med. Chem.* 2009, 44, 1010–1015.
19. G. O. Ildiz, I. Boz and O. Unsalan, FTIR Spectroscopic and Quantum Chemical Studies on Hydantoin. *Opt. Spectrosc.* 2012, 112, 665–670.
20. G. O. Ildiz, C. M. Nunes and R. Fausto, Matrix Isolation Infrared Spectra and Photo-chemistry of Hydantoin. *J. Phys. Chem. A* 2013, 117, 726–734.
21. B. A. Nogueira, G. O. Ildiz, J. Canotilho, M. E. S. Eusébio and R. Fausto, Molecular Structure, Infrared Spectra, Photochemistry and Thermal Properties of 1-Methylhydantoin. *J. Phys. Chem. A* 2014, 118, 5994–6008.
22. B. A. Nogueira, G. O. Ildiz, J. Canotilho, M. E. S. Eusébio and R. Fausto, 5-Methylhydantoin: From Isolated Molecules in a Low-Temperature Argon Matrix to Solid State Polymorphs Characterization. *J. Phys. Chem. A* 2017, 121, 5267–5279.
23. B. A. Nogueira, G. O. Ildiz, M. S. C. Henriques, J. A. Paixão and R. Fausto, Structural and Spectroscopic Characterization of the Second Polymorph of 1-Methylhydantoin, *J. Mol. Struct.* 2017, 1148, 111–118.
24. B. A. Nogueira, G. O. Ildiz, J. Canotilho, M. E. S. Eusébio, M. S. C. Henriques, J. A. Paixão and R. Fausto, Conformational Landscape and Polymorphism in 5-Acetic Acid Hydantoin. *J. Phys. Chem. A* 2020 (in the press). https://doi.org/10.1021/acs.jpca.0c03789
25. B. A. Nogueira, C. Castiglioni and R. Fausto, Color Polymorphism in Organic Crystals, *Commun. Chem.-Nature* 2020, 3, 1–12.
26. H. S. Shah, K. Chaturvedi, M. Zeller, S. Bates and K. Morris, A Threefold Superstructure of the Anti-epileptic Drug Phenytoin Sodium as a Mixed Methanol Solvate Hydrate. *Acta Crystallogr. C* 2019, 75, 1213–1219.
27. G. Sheldrick, Crystal Structure Refinement with SHELXL, *Acta Crystallogr. C* 2015, 71, 3–8.
28. M. J. Frisch, G. W. Trucks, H. B. Schlegel, G. E. Scuseria, M. A. Robb, J. R. Cheeseman, G. Scalmani, V. Barone, B. Mennucci, G. A. Petersson, et al., Gaussian 09, Revision D.01, Gaussian, Inc. Wallingford CT. 2009.
29. A. D. Becke, Density-Functional Exchange-Energy Approximation with Correct Asymptotic Behavior. *Phys. Rev. A* 1988, 38, 3098–3100.
30. C. T. Lee, W. T. Yang and R. G. Parr, Development of the Colle-Salvati Correlation Energy Formula into a Functional of Electron Density. *Phys. Rev. B* 1988, 37, 785–789.
31. A. D. McLean and G. S. Chandler, Contracted Gaussian-basis Sets for Molecular Calculations. 1. 2nd Row Atoms, *Z*=11-18. *J. Chem. Phys.* 1980, 72, 5639–5648.

32. K. Raghavachari, J. S. Binkley, R. Seeger and J. A. Pople, Self-Consistent Molecular Orbital Methods. 20. Basis Set for Correlated Wave-functions. *J. Chem. Phys.* 1980, 72, 650–54.
33. Chemcraft (version 1.8) - Graphical Software for Visualization of Quantum Chemistry Computations. https://www.chemcraftprog.com
34. M. Taş, S. Çamur, Z. Yolcu and O. Büyükgüngör, Synthesis, Crystal Structure, Spectroscopic and Thermal Properties of a Novel Complex of Hydantoin-5-acetic Acid with Co(II). *J. Inorg. Organomet. Polym.* 2013, 23, 616–620.
35. K. Robinson, G. V. Gibbs and P. H. Ribbe, Quadratic Elongation: A Quantitative Measure of Distortion in Coordination Polyhedra. *Science* 1971, 172, 567–570.
36. E. M. S. Maçôas, J. Lundell, M. Pettersson, L. Khriachtchev, R. Fausto and M. Räsänen, Vibrational Spectroscopy of Cis- and Trans-Formic Acid in Solid Argon. *J. Mol. Spectrosc.* 2003, 219, 70–80.
37. S. Lopes, A. V. Domanskaya, R. Fausto, M. Räsänen and L. Khriachtchev, Formic and Acetic Acids in Solid Nitrogen: Enhanced Stability of the Higher Energy Conformer. *J. Chem. Phys.* 2010, 133, Art. 144507.
38. M. Rozenberg, G. Shoham, I. D. Reva and R. Fausto, A Correlation Between the Proton Stretching Vibration Red Shift and the Hydrogen Bond Length in Polycrystalline Amino Acids and Peptides, *Phys. Chem. Chem. Phys.* 2005, 7, 2376–2383.

Table of Contents Graphic

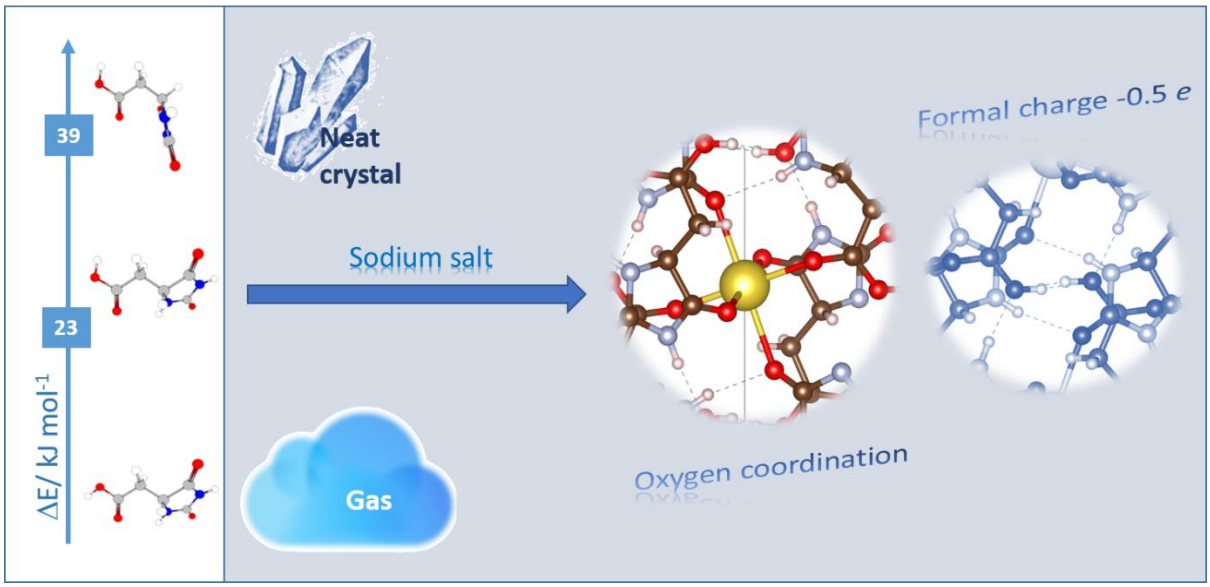

Highlights

- The sodium salt of 5AAH was synthesized and structurally characterized.
- 5AAH coordinates by O atoms (substituent and ring) in a pseudo-octahedral geometry.
- The molecular formula is $Na(5AAH)_2$; the formal charge of 5AAH in the crystal is -0.5 *e*
- The conformers of 5AAH in the crystalline salt and neat compound are distinct
- Raman spectrum of the salt was interpreted using DFT theory and data for neat 5AAH